(2)

SSS-TR-90-11535

GL-TR-90-0133

IMPLICATIONS OF EXPLOSION GENERATED SPALL MODELS: REGIONAL SEISMIC SIGNALS

K. L. McLaughlin
T. G. Barker
S. M. Day

S-CUBED
A Division of Maxwell Laboratories, Inc.
P.O. Box 1620, La Jolla, CA, 92038-1620

May 1990

Scientific Report No. 2

Approved for Public Release; Distribution Unlimited

GEOPHYSICS LABORATORY
AIR FORCE SYSTEMS COMMAND
UNITED STATES AIR FORCE
HANSCOM AIR FORCE BASE, MA 01731-5000

90

SPONSORED BY
Defense Advanced Research Projects Agency
Nuclear Monitoring Research Office
ARPA ORDER NO 5307

MONITORED BY
Geophysics Laboratory
F19628-89-C-0043

This technical report has been reviewed and is approved for publication.

JAMES F. LEWKOWICZ
Contract Manager
Solid Earth Geophysics Branch
Earth Sciences Division

JAMES F. LEWKOWICZ
Branch Chief
Solid Earth Geophysics Branch
Earth Sciences Division

FOR THE COMMANDER

DONALD H. ECKHARDT, Director
Earth Sciences Division

REPORT DOCUMENTATION PAGE

Form Approved
OMB No. 0704-0188

1. AGENCY USE ONLY (Leave blank)	2. REPORT DATE May 1990	3. REPORT TYPE AND DATES COVERED Scientific Report No. 2

4. TITLE AND SUBTITLE IMPLICATIONS OF EXPLOSION GENERATED SPALL MODELS: REGIONAL SEISMIC SIGNALS	5. FUNDING NUMBERS F19628-89-C-0043 PE 62714E PR 9A10 TA OA WU BG
6. AUTHOR(S) McLaughlin, K. L., Barker, T. G., Day, S. M.	
7. PERFORMING ORGANIZATION NAME(S) AND ADDRESS(ES) S-CUBED, A Division of Maxwell Laboratories, Inc. P.O. Box 1620 La Jolla, CA 92038-1620	8. PERFORMING ORGANIZATION REPORT NUMBER SSS-TR-90-11535
9. SPONSORING/MONITORING AGENCY NAME(S) AND ADDRESS(ES) Geophysics Laboratory Hanscom Air Force Base Massachusetts 01731 Contract Manager: James Lewkowicz/LWH	10. SPONSORING/MONITORING AGENCY REPORT NUMBER GL-TR-90-0133
11. SUPPLEMENTARY NOTES	
12a. DISTRIBUTION/AVAILABILITY STATEMENT Approved for Public Release; Distribution Unlimited	12b. DISTRIBUTION CODE

13. ABSTRACT (Maximum 200 words)

The contribution of the spall source to the short period regional explosion seismogram is studied using new parametric models for the spallation seismic source derived from (2-D) axisymmetric nonlinear finite difference simulations for underground nuclear explosions. It is concluded that in high-velocity crustal structures spall may be a significant source of short period Lg and may significantly affect the Pg excitation.

Regional phase excitation from a vertical point force and a horizontal tension crack are examined. A new general derivation for the equivalence between the two representations at low frequencies (horizontal wavelength >> spall depth) is given. Numerical calculations show that the vertical point force at the free surface above the spall is a good approximation in the short period bandwidth but degrades at high frequencies (horizontal wavelength < half the spall depth).

A smoothing operator is presented to account for the distributed finite nature of the spall. This operator represents a distributed spall disk with zero motion at the tip, and has an upward concave spall surface. It is proportional to $\omega^{-5/2}$ at high frequencies. Since the spall source is proportional to ω^2 for low frequencies, the far-field signal should be significant only for a narrow band of frequencies (0.5-2.0 Hz).

The parameterized model of Barker and Day (1990) is used to compare regional waveforms from spall and explosion sources in a high-velocity crustal model. The short-period Lg signal is completely dominated by the spall source. The spall source for a 680 m deep 125 KT explosion corresponds to a 6.2 $m_b(Lg)$ in the Stevens (1986) model for Eastern Kazakhstan. Simulations suggest that if spall is a significant source of Lg excitation then $m_b(Lg)$ should be sensitive to scaled depth of burial.

14. SUBJECT TERMS Spall, Explosion, Seismic Waveforms, Finite Difference, Regional Waveforms			15. NUMBER OF PAGES 50
			16. PRICE CODE
17. SECURITY CLASSIFICATION OF REPORT UNCLASSIFIED	18. SECURITY CLASSIFICATION OF THIS PAGE UNCLASSIFIED	19. SECURITY CLASSIFICATION OF ABSTRACT UNCLASSIFIED	20. LIMITATION OF ABSTRACT SAR

NSN 7540-01-280-5500

Standard Form 298 (Rev. 2-89)
Prescribed by ANSI Std. 239-18
298-102

TABLE OF CONTENTS

LIST OF ILLUSTRATIONS

I. SUMMARY

The contribution of the spall source to the short period regional explosion seismogram is studied using new parametric models for the spallation seismic source derived from two-dimensional (2-D) axisymmetric nonlinear finite difference simulations for contained underground nuclear explosions. It is concluded that for high-velocity crustal structures spall may be a significant source of short period Lg and may significantly affect the Pg excitation.

Two seismic source representations for spall are compared. Regional phase excitation from a vertical point force and a horizontal tension crack are examined. A new general derivation for the equivalence between the two representations at low frequencies (horizontal wavelength >> spall depth) is given. Numerical calculations show that the vertical point force at the free surface above the spall is a good approximation in the short period bandwidth but degrades at high frequencies (horizontal wavelength < half the spall depth).

A smoothing operator is presented to account for the distributed finite nature of the spall. This operator has the desirable characteristics that it represents a distributed spall disk with zero motion at the tip, has an upward concave spall surface. It falls-off proportional to $\omega^{-5/2}$ at high frequencies. Since the spall source is proportional to ω^2 for low frequencies, the far-field signal should be signficant only for a narrow band of frequencies compared to the broadband explosion signal. This narrow band can be expected to coincide with the traditional short period seismic band (0.5-2 Hz) for explosions in the 1

to 150 Kt yield ra..ge at normal depths of burial.

The parameterized model of Barker and Day (1990) is then used to examine the significance of spall signature in regional waveforms compared to the explosion contribution to the seismogram. Green's functions are computed for a high-velocity near-surface layer crustal model. It is found that for reasonable amounts of spall, the short period Lg signal is completely dominated by the spall source. The Barker and Day spall source for a 125 Kt explosion buried at 680 meter depth corresponds to a 6.2 $m_b(Lg)$ in the Stevens (1986) crustal model for Eastern Kazakhstan. The Pg signal may be dominated by the spall source for a narrower bandwidth. Simulations suggest that if spall is a *significant source of Lg excitation then* m_b(Lg) should be sensitive to scaled depth of burial.

II. INTRODUCTION

It was shown by Day, *et al.* (1983) that a proper seismic source representation for spall must conserve momentum and therefore the spall signal has no "zero" frequency source strength. Day, *et al.* then showed that for low frequency surface waves an equivalent force model for spall could be represented by a vertical point force. They demonstrated that in the low-frequency limit, the vertical opening of a horizontal tension crack is equivalent to a vertical force on the surface with a suitable time history. In recent years this spall model has been increasingly used to represent the seismic spall signal at higher frequencies than it was initially applied. Stump (1984) has shown that for the purposes of source inversion, suitable combinations of vertical point forces and explosion sources can not be distinguished from an explosion plus a tension crack. In subsequent work, Stump (1985) has used the Day, *et al.* model combined with an *ad–hoc* smoothing operator to model small contained chemical explosions. Recently, Patton (1988) has used the Day, *et al.* model as modified by Stump to model regional Rayleigh and Lg waves by moment tensor inversion for the NTS explosion HARZER. Patton concluded that the spall signal was a significant contributor to the Lg signal below 1 Hz. Johnson (1988) using near-source data performed moment tensor inversions for HARZER and another NTS explosion, CHANCELLOR, and found similar results to Patton. In both cases, it was found that a source secondary to the explosion could be represented as either a vertical point force, F_z, or an additional contributor to the vertical couple, M_{zz}. Recently, Taylor (1989) used the modified Day, *et al.*

model to argue that spall is a significant contributor to regional Pg and that depth of burial (and hence relative size of spall) influences the proposed Murphy and Bennett (1983) high/low frequency spectral ratio discriminant.

In this paper, we present a more general derivation of the vertical point force at the surface as an approximation for the buried tension crack representation. We show that the approximation is valid in a more general context than originally shown by Day, *et al.* (1983) and examine the limitations of the approximation. Green's functions for point source loads and buried tension cracks are examined in the time and frequency domain for a simple crustal structure. We see that the vertical point force approximation may suffice for many applications. However, the radiation pattern and frequency dependence of the tension crack differs from the point force at high frequencies and the tension crack representation may be a more accurate representation.

Following the discussion regarding the seismic source representation of spall, we discuss possible smoothing operators to be used to represent the finite extent of spall. A take off angle dependent smoothing operator is chosen that has reasonable high frequency behavior, zero displacement at the tension crack tip, and has a concave upward spall surface.

Finally, we examine spall modeling results of Barker and Day (1990) based on axisymmetric spall models that fit teleseismic P waves radiated by 2-D axisymmetric nonlinear finite difference explosion simulations. Regional seismograms are computed based on their spall model and the relative excitation of Pg and Lg are compared from the explosion and spall sources.

III. AN EQUIVALENT FORCE REPRESENTATION FOR SPALL

Day, *et al.* (1983) suggested that spall may be represented as a horizontally oriented tension crack that opens and closes in the vertical direction (see Figure 1). Given this simplification, we can write that the far field displacement due to the motion on a surface is given by (Aki and Richards, 1980)

$$u_i(\omega,r) = \int_\Sigma n_j(\eta)\ \delta u_k(\omega,\eta)\ C_{jkpq}(\eta)\ \frac{\partial G_{ip}(\eta)}{\partial \eta_q}\ d^2\eta \tag{1}$$

where Σ is the spall surface with unit normal, $n_j(\eta)$, and $\delta u_k(\eta)$ is the motion across the surface, $C_{jkpq}(\eta)$ is the elastic modulus tensor, and $G_{ip}(\eta)$ is the Green's tensor for the medium. For the opening of a horizontal tension crack $n(\eta)$ and $\delta u(\eta)$ are parallel in the vertical direction, j=z, and we can write, $T_{izz}(\eta) = C_{zzpq}(\eta)\ \dfrac{\partial G_{ip}(\eta)}{\partial \eta_q}$, which by reciprocity is the vertical stress component at the source location, η, due to a point force in the i'th direction at the receiver location, r. Equation (1) becomes,

$$u_i(\omega,r) = \int_\Sigma \delta u_z(\omega,x,y)\ T_{izz}(x,y)\ dxdy. \tag{2}$$

We expand T_{izz} in a Taylor expansion about the free surface, z=0,

$$T_{izz} = T_{izz}\Big|_{z=0} + z\frac{\partial T_{izz}}{\partial z}\Big|_{z=0} + \dots \tag{3}$$

By virtue of the free surface, the first term is zero, and Equation (2) becomes

$$u_i(\omega,r) = h_s \int_\Sigma \delta u_z(\omega,x,y)\ T_{izz}(x,y)\Big|_{z=0}\ dxdy \tag{4}$$

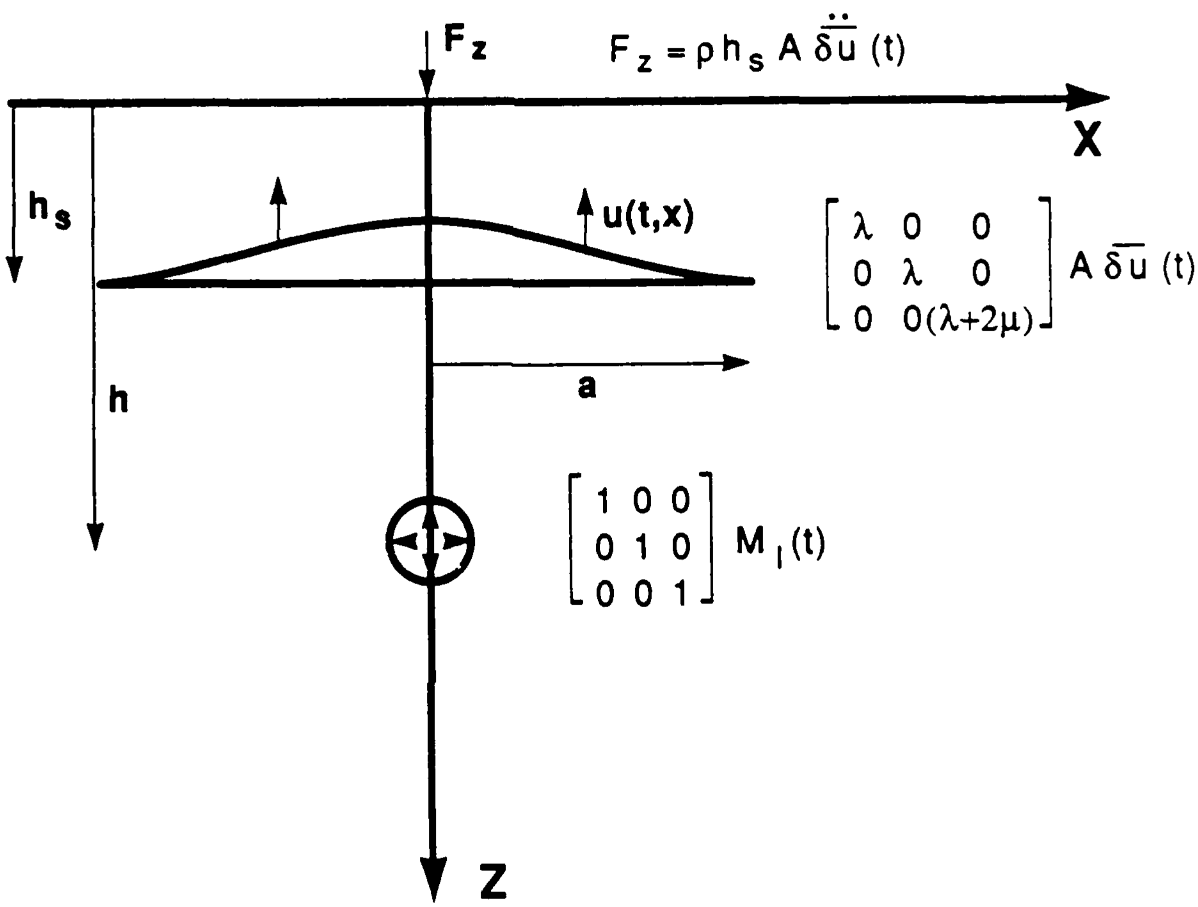

Figure 1. The axisymmetric spall above the explosion is modeled as a circular horizontal tension crack that opens and closes in the vertical direction. The spall is parameterized by the source depth h_s, the crack radius a, and the displacement time function u(t,x). The radiation from a horizontal tension crack is equivalent at low frequencies to the radiation from a vertical point force, F_z, at the surface proportional to the second time derivative of δu. The moment tensor source representation for the tension crack is proportional to δu. A is the area of the crack, ρ is the density, and λ and μ are the Lame parametes for the medium.

where h_s is the spall depth. Since T_{ijk} is the stress field due to G_{ij}, we may write the z'th component of the equation of motion,

$$\frac{\partial T_{izz}}{\partial z} + \frac{\partial T_{iyz}}{\partial y} + \frac{\partial T_{ixz}}{\partial x} = -\omega^2 \rho G_{iz}. \tag{5}$$

If we apply Equation (5) to the free surface, z=0, then the partial derivatives with respect to x and y are zero since $T_{iyz} = T_{ixz} = 0$ for z=0, and we have that,

$$\frac{\partial T_{izz}}{\partial z}\Big|_{z=0} = -\omega^2 \rho G_{iz}(z=0). \tag{6}$$

Substitute Equation (6) into Equation (4),

$$u_i(\omega,r) = -\rho h_s \omega^2 \int_\Sigma \delta u_z(\omega,x,y)\ G_{iz}(x,y,z=0)\ dxdy \tag{7}$$

$$u_i(\omega,r) \ = \ -\rho h_s A \omega^2 \overline{\delta u_z} G_{iz} = -m_s \omega^2 \overline{\delta u_z} G_{iz} = i\omega I_s G_{iz}. \tag{8}$$

Thus, $-\rho h_s \omega^2 \delta u_z(\omega,x,y)$ is interpreted as the vertical force per unit area at the free surface, z=0. Note that the equivalent force is applied to the free surface above the spall surface, and that the force has the time history of the spall acceleration. In contrast, the tension crack source has the time history of the spall displacement. The spall momentum, I_s, is given by the spall mass, $m_s = \rho h_s A$, times the mean velocity, $i\omega\overline{\delta u_z}$ and therefore the equivalent spall force, $F_s = i\omega I_s$. In this manner we can relate estimates of spall mass, and momentum to an equivalent point force. Alternatively, we could use Equation (2) to describe the source as a buried tension crack,

$$u_i(\omega,r) = \overline{\delta u_z} A T_{izz} = \overline{\delta u_z} A[\lambda G_{ix,x} + \lambda G_{i,yy} + (\lambda+2\mu) G_{iz,z}] \tag{9}$$

There are several approximations inherent in the derivation of Equation (7). Since a Taylor expansion was used from the free surface, it is likely that the representation will break down for seismic wavelengths on the order of the spall depth. Related to this limitation is the fact that the radiation pattern for a point force at the free surface is not exactly the same as that for a tension crack at depth.

We address these two limitations by comparing the regional Green's functions for a surface point force and the buried horizontal tension crack. Equations (8) and (9) imply that $\rho h_s \omega^2 G_{iz}(z=0) \approx T_{izz}(z=h_s)$. Figure 2 shows the Green's functions for buried tension cracks compared to the Green's function for a vertical point force at the free surface. The Green's functions were computed for the vertical displacement at a distance of 300 km using the Eastern Kazakhstan crustal model from McLaughlin, *et al.* (1988) (see Table 1). A wavenumber integration code was used to compute the full response of the medium from 0 to 5 Hz. The tension crack ($T_{zzz}(t)$) and vertical point force ($\rho h_s \ddot{G}_{zz}(t)$) Green's functions are all plotted to the same scale. We see that the relative amplitudes of the Pg, Lg, and Rg are similar when we compare the point force and tension crack representations for depths less than 500 m. However, the individual wavepackets in the Pg can be seen to vary with depth for the tension crack sources.

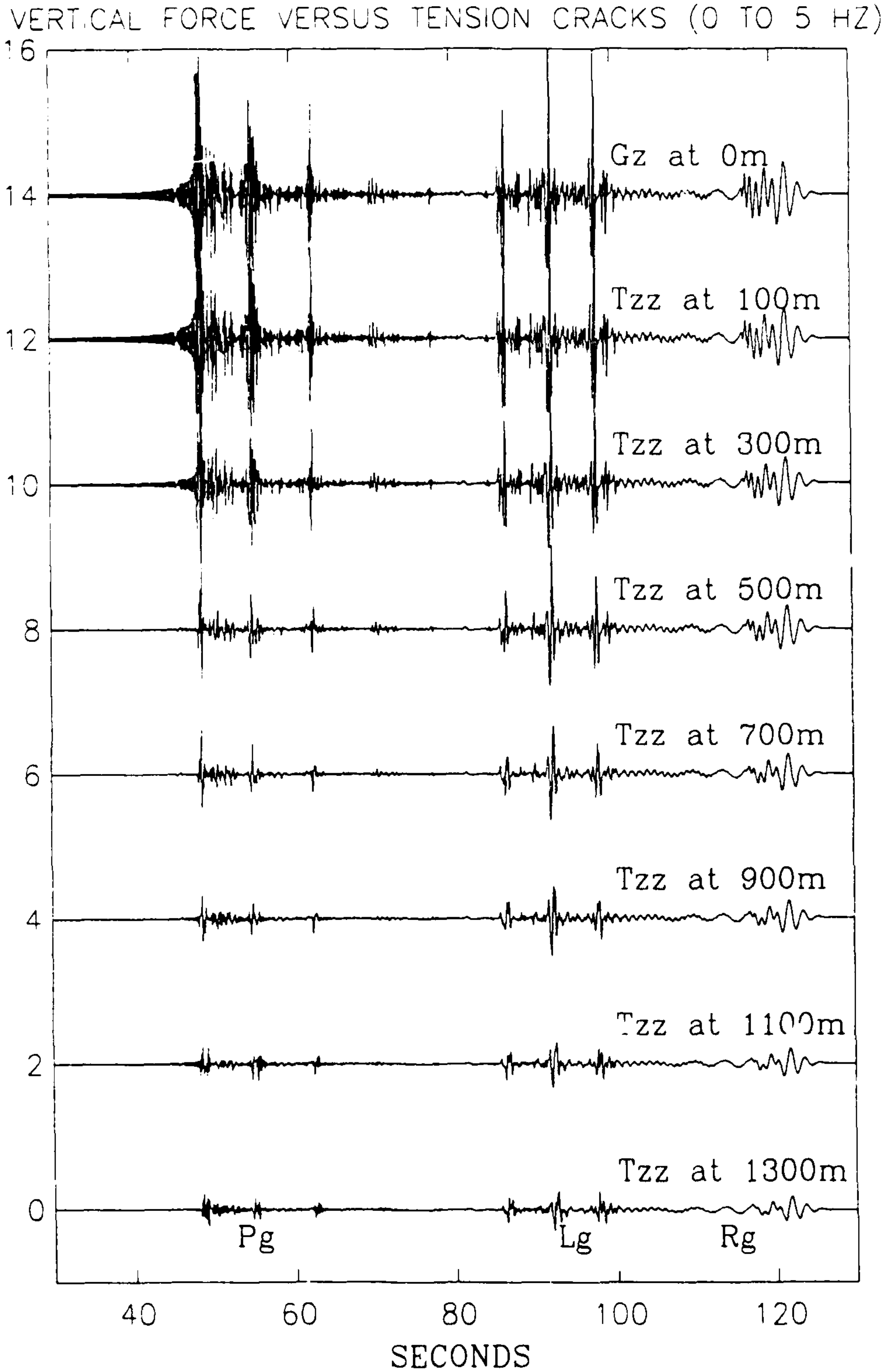

Figure 2. The broadband (0 to 5 Hz) vertical displacement at a distance of 300 km due to a vertical point force at the surface is compared to that motion due to tension cracks at depth. Pg, Lg and Rg wavepackets are indicated. Similarity of waveforms degrades for depth > 300 m in this bandwidth (0-5 Hz).

TABLE 1.
Eastern Kazakhstan Structure Modified from Stevens (1986)

h(km)	α(km/s)	β(km/s)	ρ(gm/cc)	Q_μ	depth(km)
2.000	5.020	2.790	2.700	100.0	0.000
1.000	5.400	3.000	2.700	150.0	2.000
2.488	5.900	3.300	2.700	200.0	3.000
10.976	6.100	3.400	2.700	600.0	5.488
5.488	6.308	3.541	2.702	525.9	16.464
5.488	6.597	3.703	2.807	500.0	21.952
5.488	6.736	3.781	2.858	450.0	27.440
5.564	6.782	3.807	2.875	400.0	32.928
6.504	6.795	3.814	2.879	350.0	38.492
8.006	8.147	4.573	3.372	179.5	44.996
9.359	8.138	4.568	3.369	167.5	53.002
10.940	8.106	4.550	3.358	159.4	62.361
12.780	8.065	4.527	3.343	153.8	73.301
14.950	8.047	4.517	3.336	150.3	86.081
17.470	8.070	4.530	3.345	148.7	101.031
20.420	8.117	4.556	3.361	148.1	118.501
23.880	8.154	4.577	3.375	147.9	138.921
27.910	8.161	4.581	3.378	147.4	162.801
32.630	8.145	4.572	3.372	146.8	190.711
38.140	8.120	4.558	3.363	146.2	223.341
∞	8.101	4.547	3.356	145.8	261.481

Figure 3 shows an enlargement of the Pg waveforms in Figure 2. A visual comparison shows that correct phasing occurs between the point force and the tension crack sources for low frequencies while differences are most pronounced at high frequencies and greater depths due to interference effects between pP and P components of the Pg wavetrain.

To illustrate this further, Figure 4 compares the point source and buried tension crack sources in the frequency domain for windows taken around the Pg, Lg, and Rg phases. We see that the shallowest tension crack (100 m) is well represented by a point force up to 5 Hz for the Pg, Lg, and Rg. Modulation of the 700 m tension crack source is clearly present in the Lg ratio due to sS+S interference. It appears that the vertical point force representation is a good approximation to the buried tension crack at least up to spall depths of 1/2 the wavelength. For spall depths of 500 meters this corresponds to about 5.0 Hz for P waves in this model and about 2.8 Hz for S waves. For this velocity structure the differences at several slownesses (Pg, Lg, and Rg) between the tension crack and vertical point force representation are probably not significant below 5 Hz for spall depths shallower than 300 m.

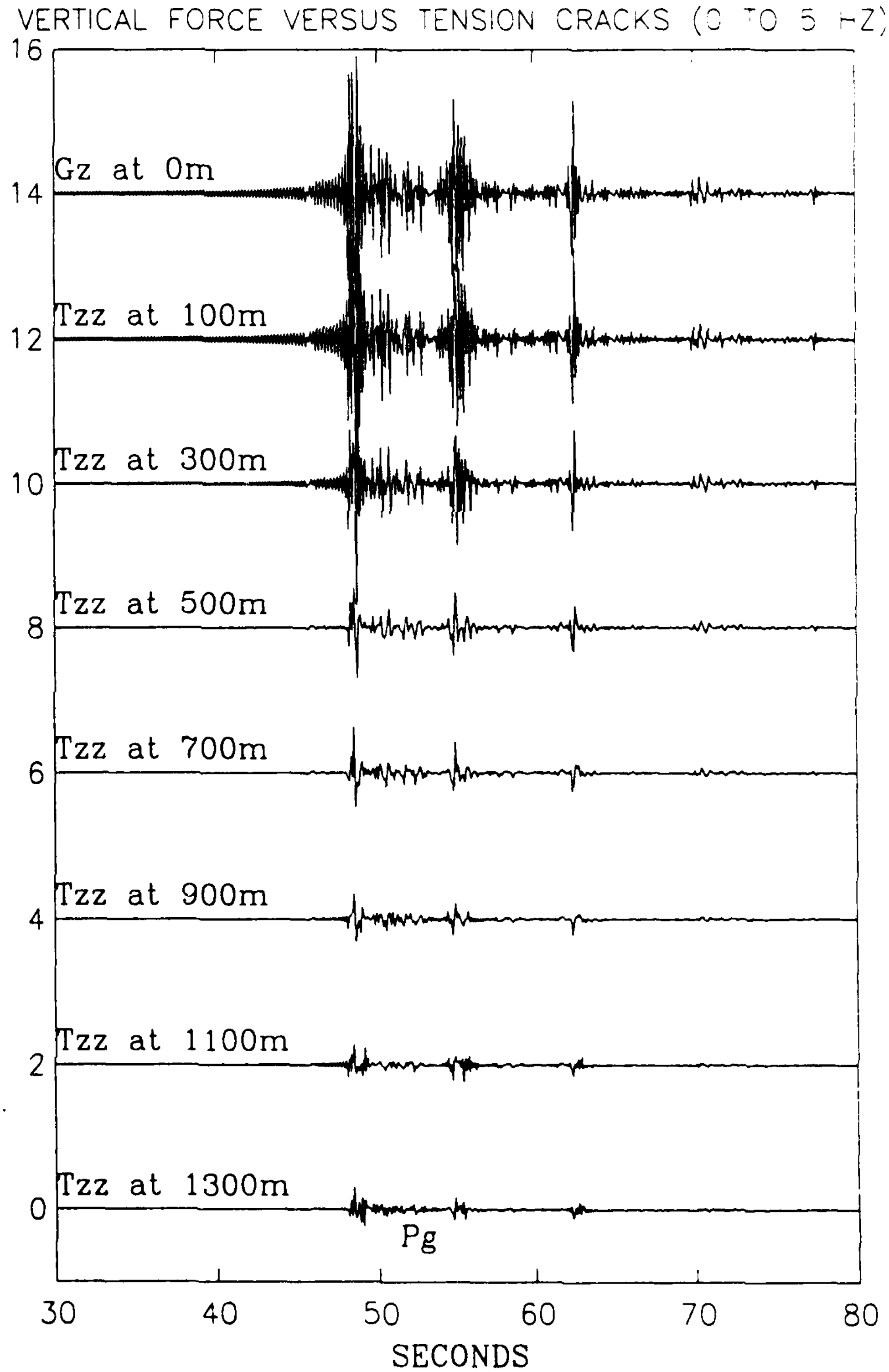

Figure 3. An enlargement of the Pg waveforms of Figure 2. Note that the similarity of the waveforms degrades for depth > 300 m.

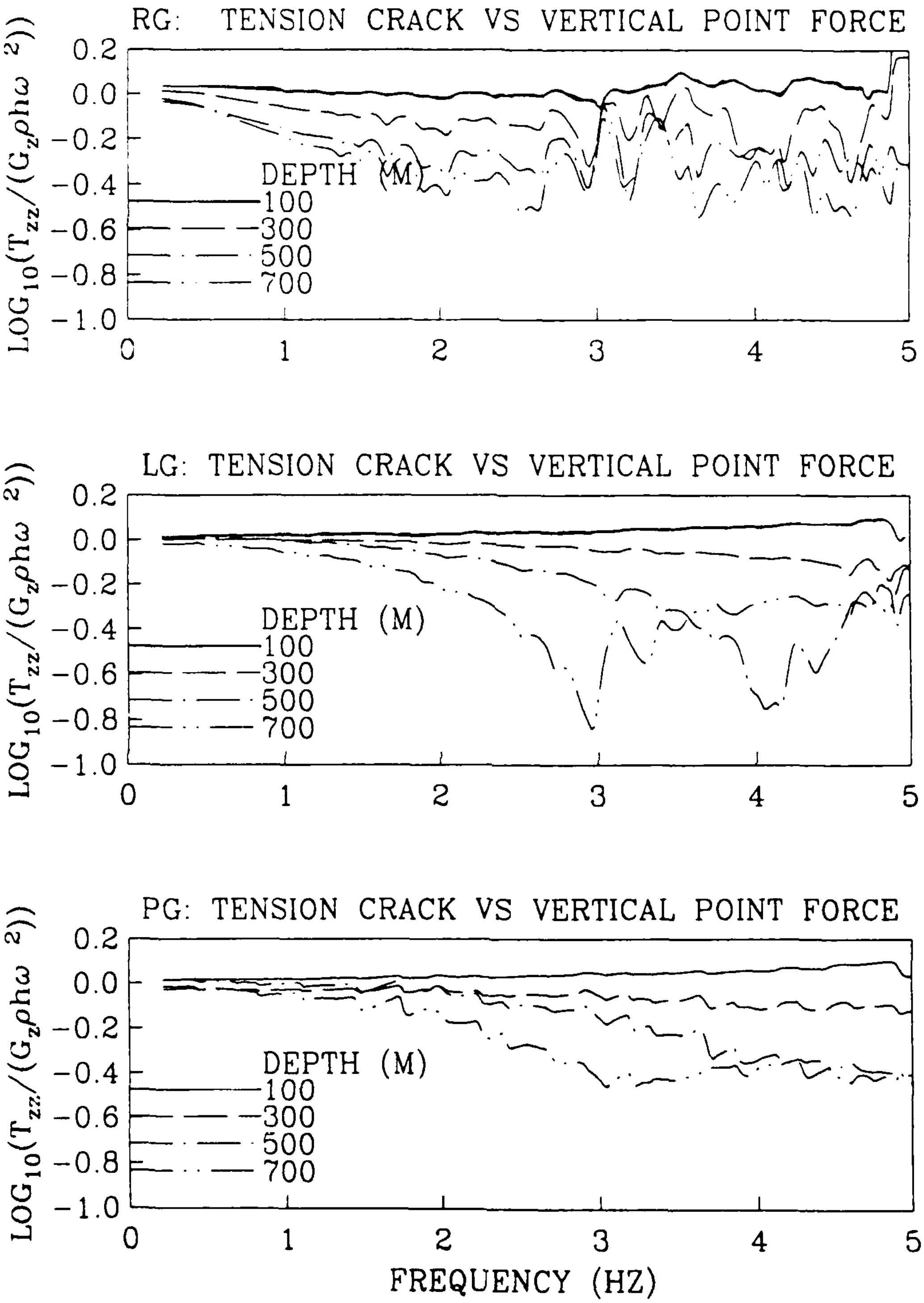

Figure 4. Spectral ratios of the tension crack seismograms over the vertical point force seismogram of Figure 2. Windows were taken around the Pg, Lg and Rg phases. Tension crack seismograms for source depths of 100, 300, 500 and 700 m are shown. In general, the approximation of the tension crack by the vertical point force degrades with depth of the tension crack.

IV. THE FINITE EXTENT OF SPALL

At high frequencies, the distributed nature of spall is not adequately represented by a single point force on the surface or even by the moment tensor representation of a tension crack. We wish to derive some simple expressions for the high frequency asymptotic behavior of the spall signal in the far field. Suppose that the spall displacement is specified over a disk of radius, a, then for a wavepacket with horizontal wavenumber, $k = \omega \frac{sin(\phi)}{c}$, where ϕ is the incidence angle, the far field displacement at range, r, will be approximated by

$$u_i(\omega,r,k) \approx U_i(\omega,r,k) \int_{\Sigma} S(\omega,x,y)e^{-ikx}dxdy \tag{10}$$

$$= U_i(\omega,r,k) \int_0^{2\pi}\int_0^a S(\omega,s,\theta)e^{-iks\cos(\theta)}sdsd\theta$$

$U_i(\omega,r,k)S(\omega,s,\theta)$ describes the contribution to the seismogram with horizontal wavenumber k from a location on the spall disk. If we assume that $U_i(\omega,r,k)S(\omega,s,\theta)$ is independent of θ then we have a zero'th order Hankel transform of the form,

$$u_i(\omega,r,k) \approx U_i(\omega,r,k)\ 2\pi\int_0^a S(\omega,s)J_0(ks)sds. \tag{12}$$

If we assume that $U_i(\omega,r,k)S(\omega,s,\theta)$ is uniform over the disk then we have

$$u_i(\omega,r,k) \approx U_i(\omega,r,k)\frac{2\pi a^2}{(ka)}J_1(ka) = U_i(\omega,r,k)E(k), \tag{13}$$

where $J_1(.)$ is the 1'st order Bessel function. For large ka, E(k) is approximated by $\sqrt{2/\pi}a^{3/2}(ka)^{-3/2}\cos(ka-3\frac{\pi}{4})$. Therefore, this smoothing function imposes an

$\omega^{-3/2}$ asymptotic roll-off at high frequencies.

A convenient form for the spall distribution is $S(\omega,s) = (a^2-s^2)/a^2$, since it has zero displacement at the crack tip and the spall separation is concave upward. Under this assumption the smoothing function has spectral form,

$$E(k) = \frac{4\pi a^2}{(ka)^2} J_2(ka), \tag{14}$$

which is proportional to the 2'nd order Bessel function and for large ka rolls-off like $\omega^{-5/2}$. This simple model is preferred becasue it has the physically reasonable property of zero displacement at the crack tip, and the spall surface is concave upward as suggested by Eisler and Chilton (1964). Because this continuous spall distribution function is zero at the crack tip the smoothing operator falls off faster than ω^{-2} at high frequencies. Given the sparsity of information regarding the radial dependence of spall, this simple model will suffice to compare the relative importance of the seismic spall source with that of the explosion source. It should be noted that any simple continuous distribution function with zero at the crack tip will fall-off faster than ω^{-2} at high frequencies and therefore the far-field signal at high frequencies should be dominated by the explosion source.

V. SPALL SIGNAL SYNTHETICS

Barker and Day (1990) have used teleseismic P waves predicted by 2-D axisymmetric nonlinear finite difference simulations of explosions to derive parametric models for the equivalent spall source. They found that the differences between the nonlinear simulations and linear point explosion sources could be modeled by a simple parametric spall model. Their model is a circular horizontal tension crack of radius, a, depth, h_s, and has a uniform initial velocity distribution between v_1 and v_2. The reader is referred to Barker and Day for a detailed motivation of the model. The function $\delta\overline{u}(t)$ appropriate for use in Equations (8) or (9) is given by

$$\delta\overline{u}(t) = t(v_2 + v_1)/2 - gt^2/2, \qquad 0 \le t \le \frac{2v_1}{g} = t_1 \tag{15}$$

$$\delta\overline{u}(t) = \frac{t(v_2 - gt/2)^2}{2(v_2 - v_1)}, \qquad \frac{2v_1}{g} = t_1 < t \le \frac{2v_2}{g} = t_2$$

The 2-D nonlinear axisymmetric finite difference simulations are described in McLaughlin, *et al.* (1988) and are intended to simulate 125 Kt explosions at 200, 300, 680, and 980 meter depths in a Shagan River Test Site structure. We concentrate on the 680 and the 980 meter depth of burials which correspond to roughly normal scaled depth of burial (122 m/$Kt^{1/3}$) and 60% overburied (196 m/$Kt^{1/3}$) respectively. The spall parameters determined by Barker and Day are listed below in Table 2. Figure 5 shows the equivalent spall sources for the 680 m depth simulation as determined by Barker and Day (1990) for teleseismic P, and regional Pn, Pg, and Lg. The smoothing operator

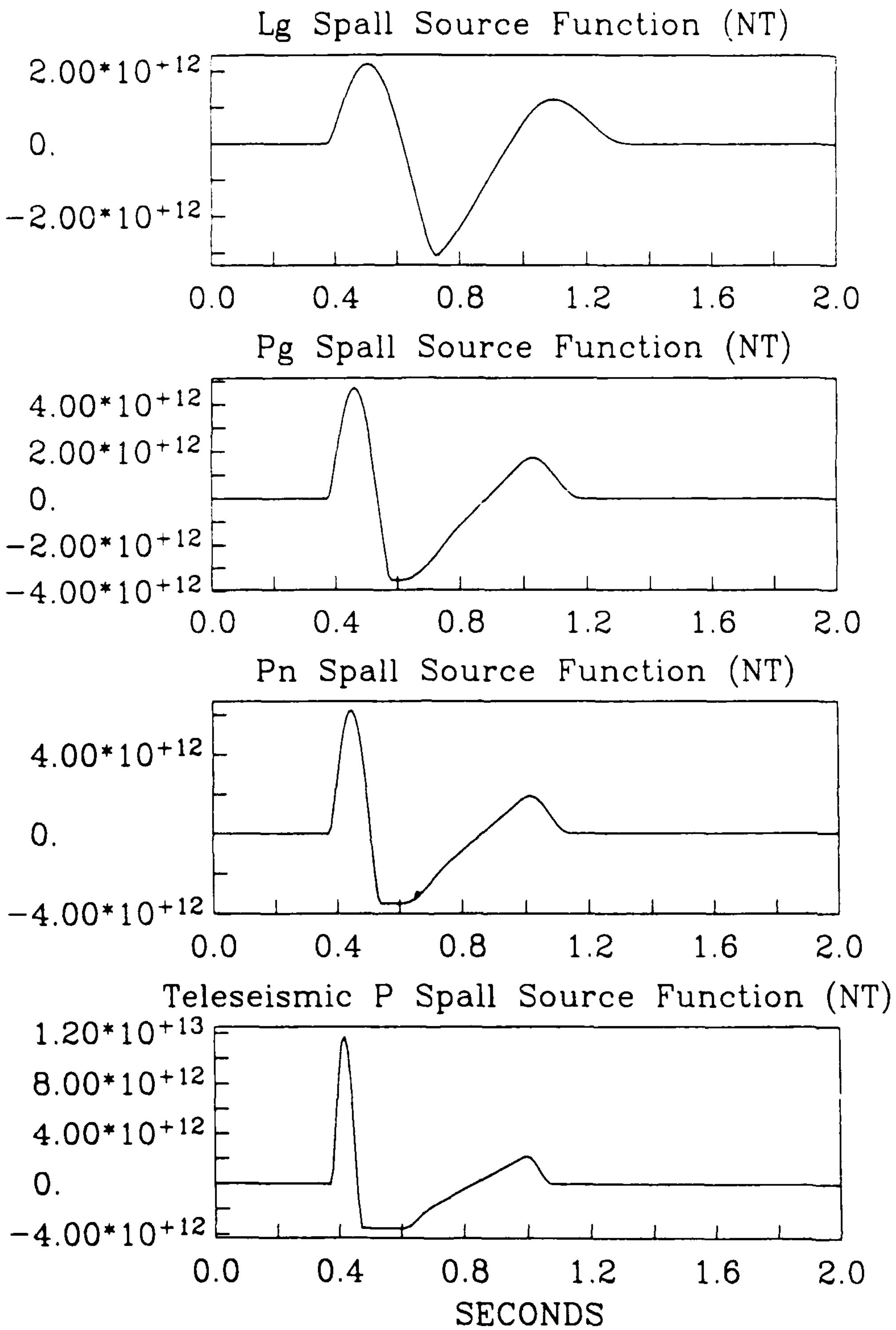

Figure 5. The equivalent spall source (for source depth of 680 m from Table 2) for four different apparent phase velocities corresponding to teleseismic P, Pn, Pg, and Lg. The smoothing operator E(t) simulates the distributed nature of the source. Slower phases are more sensitive to the size of the spall disk.

of Equation (14) was used to model the finite extent of the spall surface while the spall source time function was specified by Equation (15). Apparent velocities of 14, 8.2, 6.5, and 3.7 km/s were chosen to represent the teleseismic P, Pn, Pg, and Lg respectively. Note that the spall is characterized by a high frequency opening pulse followed by a low frequency unloading and a small spall closure pulse. Because this spall model opens simultaneously over the entire spall disk but distributes the closure, the spall closure pulse is small compared to the opening pulse.

The Lg and Pg spall sources are smoother and lower frequency than the Pn and teleseismic P spall sources. The lower the apparent velocity of the seismic phase, the more important the extended size of the source. Spectra are shown in Figure 6. We see that the model predicts a sharply peaked source spectrum for the regional phases and in particular the Lg falls-off very rapidly for frequencies above 2 Hz.

TABLE 2.
Barker & Day (1990) Spall Models for Shagan River Synthetics

source depth (m)	200	300	680	980
v_1 (m/s)	1.1	1.1	1.1	1.1
v_2 (m/s)	14.	12.	3.	1.3
a (m)	600	625	650	650
h_s (m)	100	150	200	200
I_s (10^{12} Nt-s)	2.31	3.26	1.47	0.86

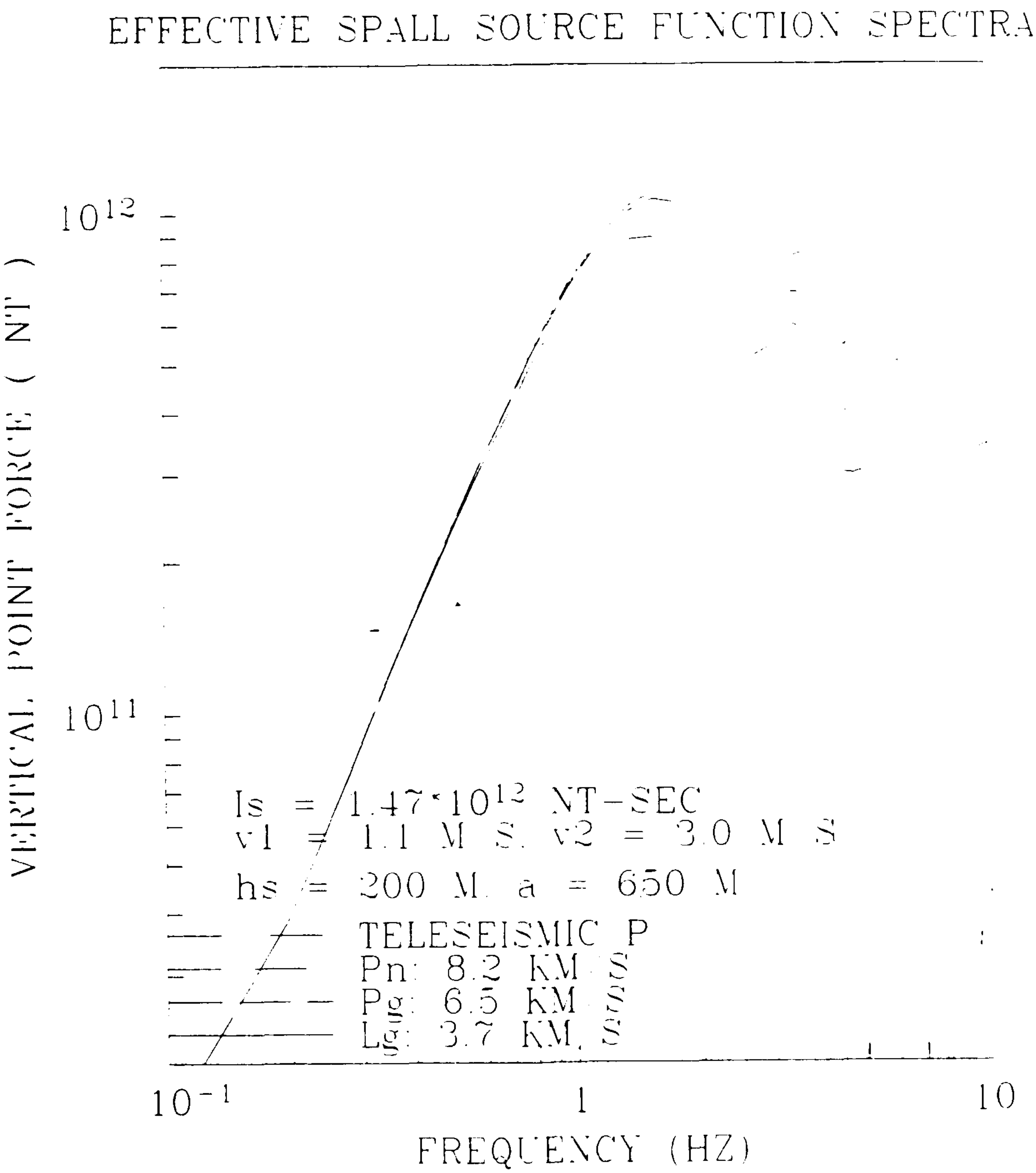

Figure 6. Spectra of the time series of Figure 5. Note that the Lg equivalent spall source falls-off more rapidly than the Pg or Pn spall source.

Figure 7 shows the tension crack Green's function for a distance of 300 km convolved with the appropriate Pg and Lg spall source functions compared with the explosion Green's function and the appropriate explosion RDP. Note that the Lg explosion signal is insignificant compared to the Lg spall signal. Based on Nuttli's (1986) formulas, $m_b(Lg)$ = 6.2 for the synthetic spall+explosion Lg signal using Q = 350, and f = 1 Hz. In contrast, the explosion synthetic $m_b(Lg)$ is 4.9. Given Nuttli's NTS $m_b(Lg)$:yield formulas the total Lg excitation is about twice as large as would be predicted for a 125 Kt NTS explosion.

It should be emphasized that the explosion source is located in a high-velocity (α > 4500 m/s) layer. The phase velocities of Lg are less than the P-wave velocity of the source medium and the explosion is an inefficient source for Lg in such a model. The explosion is a more efficeint source of Lg for a low-velocity medium such as NTS (see Barker, *et al.* 1990).

In comparison to the Lg, the raw displacements of the Pg spall and explosion signals are of the same order of magnitude. Spectra of the Pg and Lg signal windows are compared in Figure 8. The spall contribution dominates the Lg signal up to 3 Hz. At 1 Hz the spall contribution to Lg is 20 times larger than the explosion contribution. At 1 Hz, the Pg spall contribution is about twice as strong as the explosion part. The explosion source dominates the Pg signal above 1.5 Hz.

If we compare the Barker and Day spall model with other published spall sources, we find that it is intermediate in strength. Viecelli (1973) found for

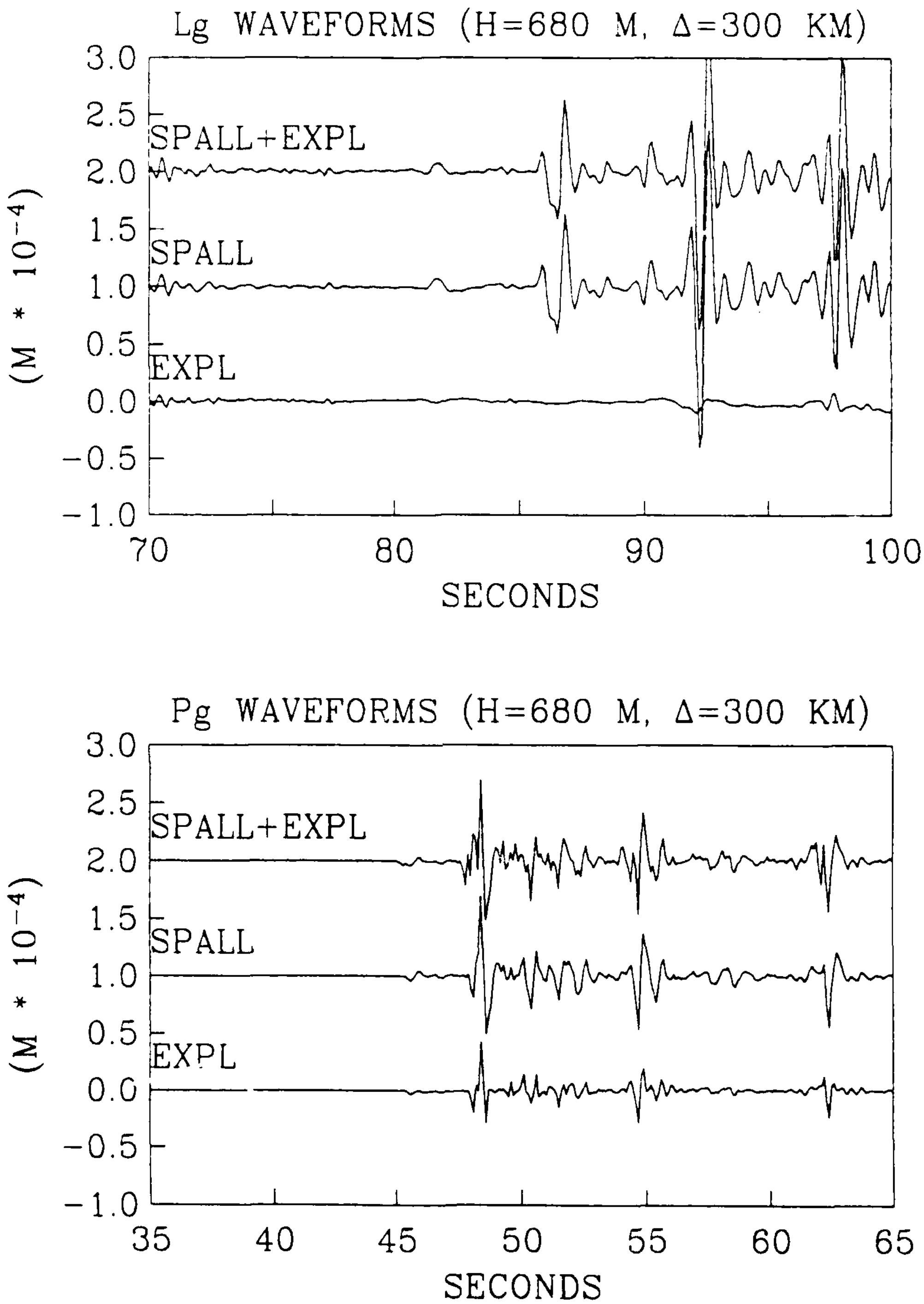

Figure 7. Synthetic Lg and Pg waveforms at a distance of 300 km for the 680 meter depth of burial 125 KT simulation. Note that the Lg spall signal dominates the Lg explosion signal while the Pg spall signal is slightly larger than the explosion Pg signal.

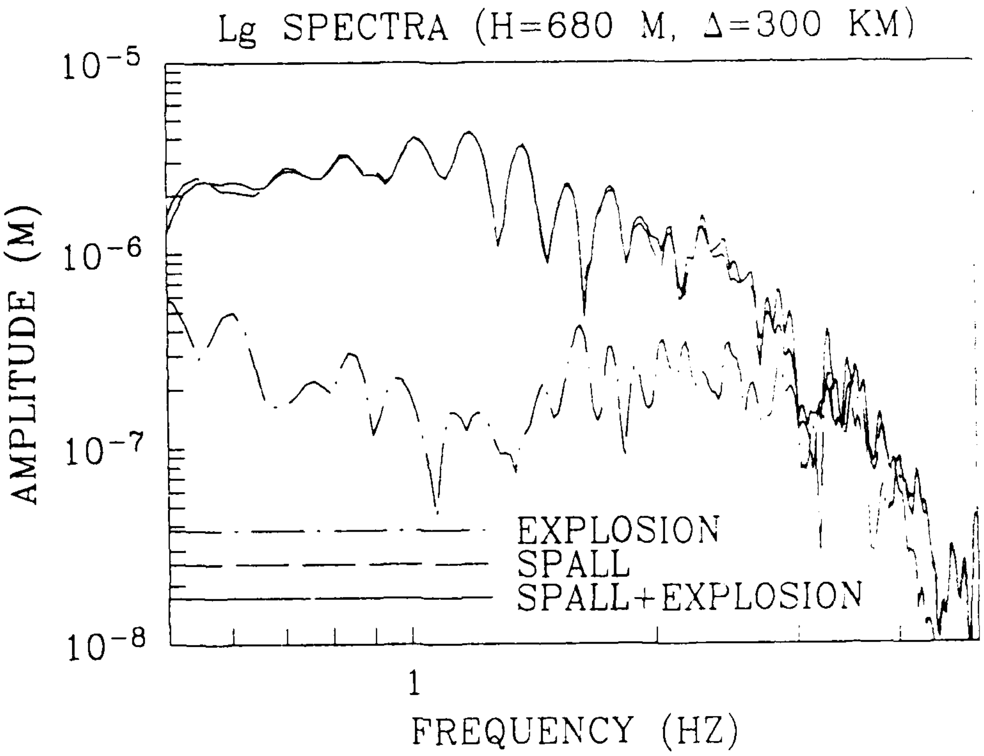

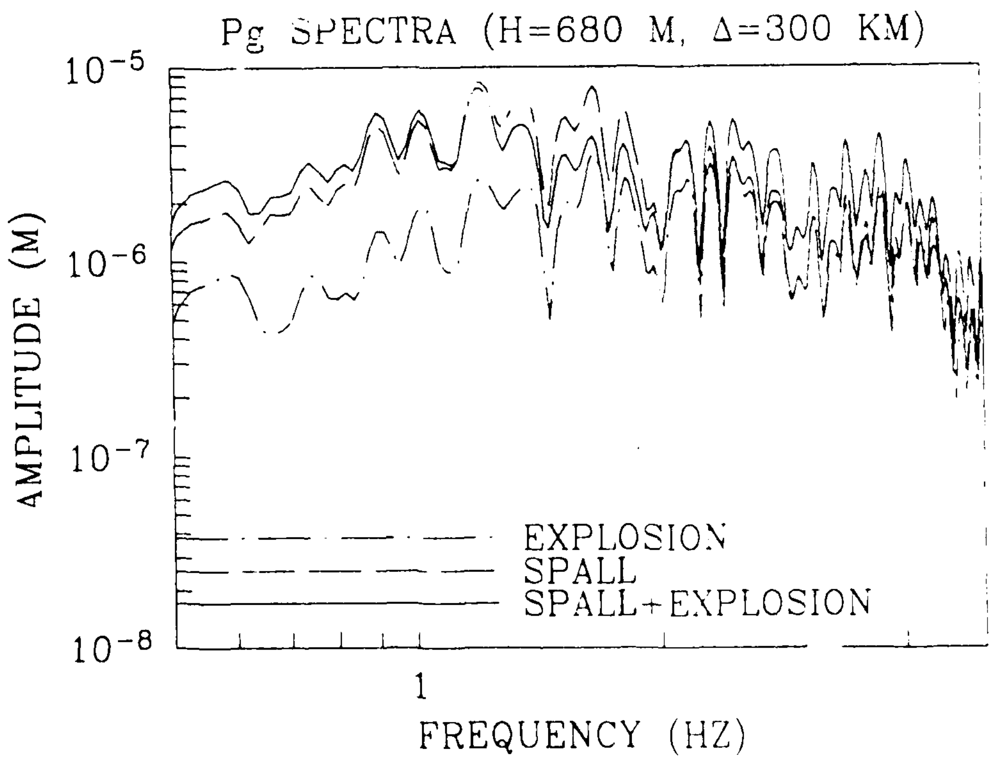

Figure 8. Spectra of the time series in Figure 7. Note that the Lg spall signal is 20 times larger than the Lg explosion signal at 1 Hz and the Pg spall signal is about two times larger than the explosion Pg signal at 1 Hz.

explosions at normal scaled depth of burial that spall momentum scaled linearly with yield as $4.6*10^9$ Nt-s/Kt. The Barker and Day spall model for the 680 meter depth of burial corresponds to about 2.5 times the spall predicted by Viecelli's scaling relationship. This is about the same factor found between Viecelli's scaling relationship and the 2-D nonlinear finite difference PILEDRIVER simulations described in Day, *et al.* (1983). Sobel's (1978) scaling relationships predict spall momenta several times larger than the Barker and Day model. It appears that the 2-D Shagan River nonlinear simulations predict spall momenta roughly intermediate between the Viecelli (1971) and Sobel (1978) scaling relationships.

Patton (1988) estimated spall momentum for the Pahute Mesa, NTS, explosion HARZER, to lie between 1 and 2 * 10^{12} Nt-s with an explosion moment between 7 and 5.7 * 10^{15} Nt-m. The simulation shown in Figures 7 and 8 had an explosion moment of about 1.4 * 10^{16} Nt-m. The spall momentum for the simulation is therefore a factor of about two lower than Patton's estimate for HARZER based on simple linear moment scaling.

Figures 9 and 10 show the Lg and Pg waveforms and their spectra for the 980 meter depth of burial simulation using the spall parameters listed in Table 2. Note that in comparison to the 680 meter depth of burial calculation, the 980 meter deep explosion contribution to Pg is larger than the spall contribution. The spall produces only 5 to 7 times more Lg at 1 Hz than the explosion, and the bandwidth is narrower for which spall is a greater source of Lg than the explosion. The total Lg amplitude at 1 Hz for the 980 meter depth of burial is

one-fourth the Lg amplitude for the 680 meter simulation.

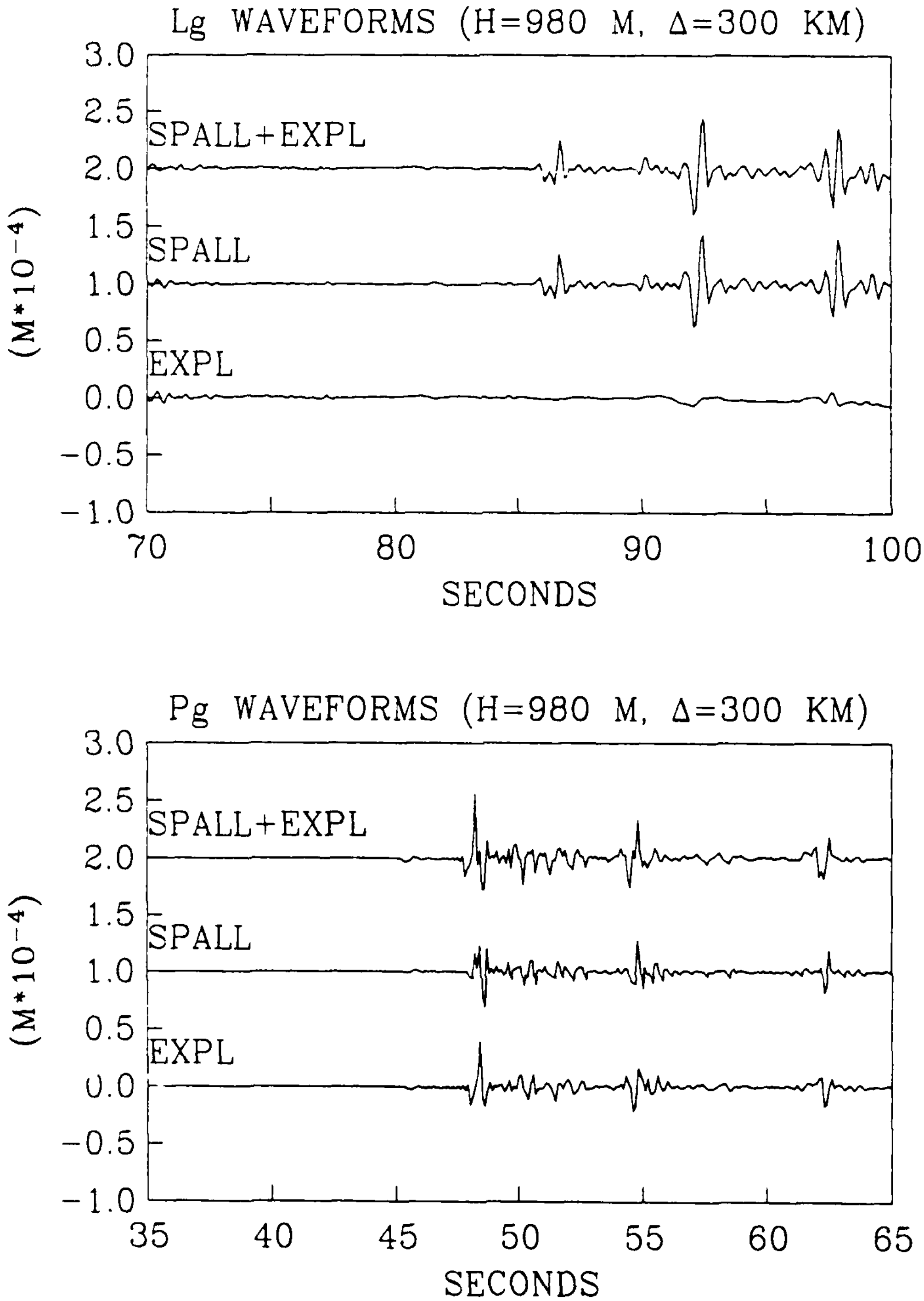

Figure 9. Synthetic Lg and Pg waveforms at a distance of 300 km for the 980 meter depth of burial 125 KT simulation. The Lg spall signal dominates the Lg explosion signal while explosion Pg signal is slightly larger than the spall Pg signal.

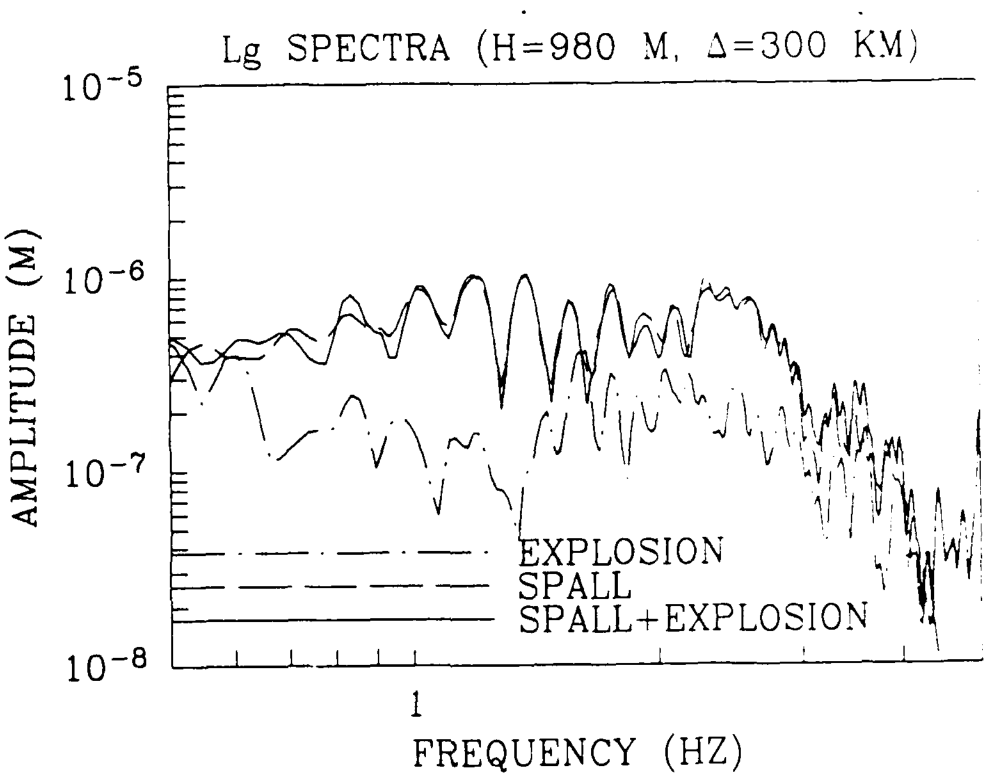

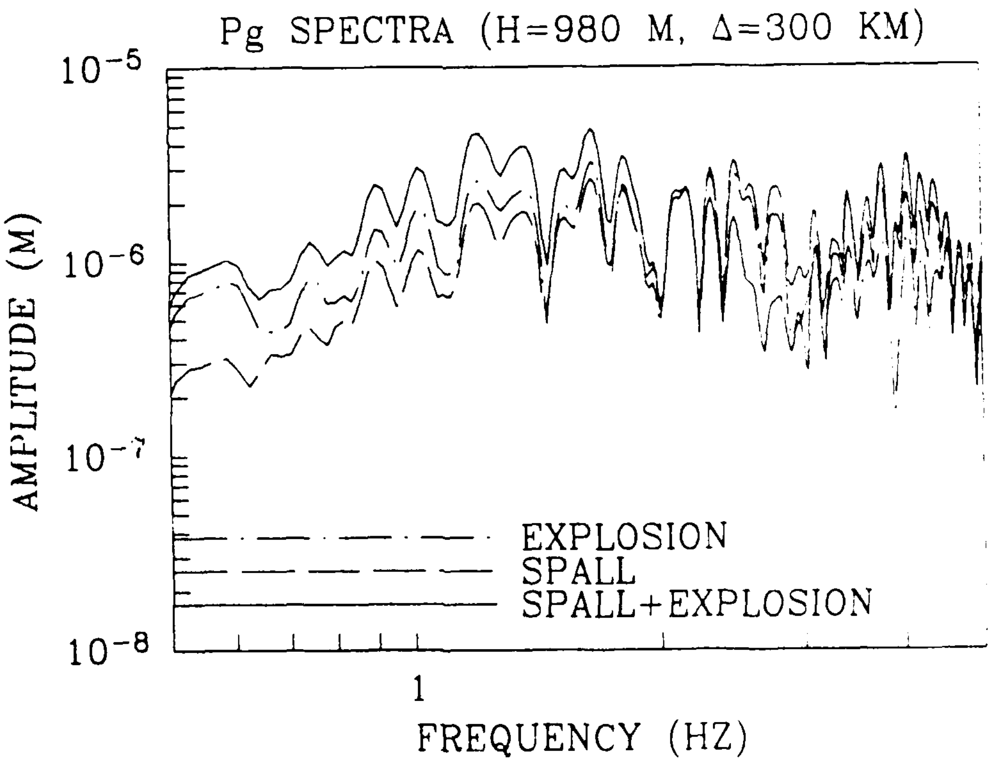

Figure 10. Spectra of the time series in Figure 9. Note that the Lg spall signal is about 5 to 7 times larger than the Lg explosion signal, while the explosion Pg signal is larger than the spall signal at nearly all frequencies.

DISCUSSION AND CONCLUSIONS

We have presented a more general derivation that a vertical point force at the surface may approximate the source of seismic radiation for a buried tension crack. The approximation was tested for a simple velocity structure, and it was found valid for frequencies up to 5 Hz, and spall depths shallower than 500 meters. One caveat to this conclusion is that the Green's functions were computed for a fairly high velocity structure with a thick surface layer. The frequencies for which the approximation is valid may be lower for lower velocity source structures or more complicated velocity structures.

A smoothing operator that simulates the distributed nature of the spall was presented. The smoothing operator (filter) has the desirable characteristics that it has zero motion at the crack tip, and the spallation surface is concave upward, therefore the spectrum falls-off at high frequencies faster than ω^{-2}. A specific model is presented that falls-off at high frequencies proportional to $\omega^{-5/2}$. Because the spall signal is proportional to ω^2 for low frequencies, the spall signal is expected to be a narrow band signal compared to the main explosion signal.

The spall model and parameters of Barker and Day (1990) were used to synthesize regional waveforms for Pg and Lg and the spall contribution to the seismogram was compared to the point explosion contribution. The Lg and Pg signals were found to be significantly affected by the spall source for the 2-D axisymmetric nonlinear finite difference simulations.

We reach a conclusion similar to Taylor (1989) that spall is probably a significant contributor to the *regional* Pg signal. This is not unexpected since spall partially cancels the pP and replaces it with a lower frequency and delayed spall signal. In addition we conclude that spall is almost certainly a significant contributor to the Lg signal for high-velocity crustal structures. It is important to note that for explosions in a low-velocity (α < 4500 m/s) near-surface layer, the explosion excitation of Lg is more efficient. The relative excitation, explosion versus spall, of Lg is not as divergent in a low-velocity source structure as in a high-velocity source structure. These conclusions require adjustment for NTS structures (see Barker, *et al.* 1990).

It should be noted that the spall model used in this paper contains approximations and lacks characteristics that should become important at higher frequencies (>5 Hz) than were examined in this paper. First of all, the spallation does not occur across a simple surface. The spall is distributed over a volume and therefore the spall parameters (v_1, v_2, h_s, a) represent integrals over a non-linear volume. Caution should be used in making too detailed physical interpretations of these model parameters. Second, the entire spall surface does not open simultaneously. This will further smooth the initial spallation signal. Third, the spall is not axisymmetric and it may radiate SH waves as well as have non axisymmetric radiation patterns for P and SV waves.

It is clear from our simulations that the spall source will depend on scaled depth of burial. Overburied explosions will tend to spall less mass for a shorter time and hence have a smaller amplitude and higher frequency spall signature.

We should expect that spall scaling will also depend on material properties and structure above the emplacement as well as the properties of the rock near the working point. Since the effects of gravitational forces on containment do not scale linearly with yield, we also expect that spallation may be more important for smaller explosions. For example, Stump (1985) found for chemical explosions in alluvium, that the spall mass was 2 to 3 times larger than that predicted by Sobel's scaling relationship. This may have been due to either weaker material properties or lack of linear scaling of gravitational effects with yield.

The m_b(Lg) predicted for the normal buried simulation (Figure 7) is roughly 0.6 to 0.7 magnitude units larger than the m_b(Lg) predicted for the 60% over buried simulation (Figure 8). If spall is the dominant source for Lg excitation then we should expect m_b(Lg) to depend upon scaled depth of burial. However, given the robust nature of m_b(Lg):yield, it is likely that other mechanisms are responsible for at least some of the Lg excitation.

The presence of transverse Lg from explosions implies that non axisymmetric nonlinear mechanisms or scattering are also responsible for Lg excitation. Although non axisymmetric spall may excite transverse Lg (Lg-SH), it has been argued by Gupta and Blandford (1983) that the Lg-SH signal grows relative to the vertical and radial components of Lg (Lg-SV) out to a couple of hundred km. This may imply that scattering is operating along the path but does not in itself explain the initial excitation of Lg-SV. Conversion of compressional energy may be converted at interfaces with significant velocity contrasts besides the free surface. Or, scattering by near source lateral heterogeneity may

contribute to the excitation of Lg and Lg-coda.

A number of overburied explosions have excited Lg as efficiently as normally buried explosions. These explosions have been located in diverse geologic environments at scaled depths of burial greater than normal containment depth ($\approx$120 $m/Kt^{1/3}$) and include SCOTCH (180 $m/Kt^{1/3}$ in tuff), REX (250 $m/Kt^{1/3}$ in tuff), SALMON (475 $m/Kt^{1/3}$ in salt), GNOME (250 $m/Kt^{1/3}$ in salt), RULISON (750 $m/Kt^{1/3}$ in shale), GASBUGGY (420 $m/Kt^{1/3}$ in shale), and RIO BLANCO (>420 $m/Kt^{1/3}$ in sandstone) (yields and depths from Springer and Kinnaman, 1971 and 1975). Nuttli (1986) has estimated the yields of six of these events to within 50% based on $m_b(Lg)$, and Blandford, *et al.* (1981) have shown that the relative Lg excitation from GNOME and SALMON is consistent with their yield ratio. The Lg excitation by these seven events argues that there are other mechanisms that contribute to Lg since spall was reduced for these explosions. A number of these events were located in geologically complicated environments and scattering may have been important (SALMON, GNOME) for some of the events. Events at NTS (SCOTCH and REX) were detonated in low-velocity materials (α < 4500 m/s) and the relative Lg contribution of spall and explosion is more nearly equal in an NTS structure. RIO BLANCO consisted of three 30 Kt explosions separated by 120 m and therefore the nonlinear zone may have deviated from spherical symmetry which would have introduced a CLVD component to the source and excited Lg. Furthermore, moderate spall was documented for RIO BLANCO by Toman *et al.* (1973). Murphy and Archambeau (1986) argue that RULISON was contaminated by

tectonic release in the short-period frequency band and the Lg excitation may reflect this deviatoric source. Murphy and Archambeau also found it necessary to incorporate spall into the modeling of teleseismic P waves for GASBUGGY and RULISON even though these events were overburied. In addition, GASBUGGY and RULISON were detonated in layered material with P-wave velocities less than or equal to 4500 m/s so the explosion source could excite Lg directly. Consequently, there appear to be no clear cut cases where an overburied explosion, uncontaminated by non-spherical effects, was detonated in high-velocity layered rock for which we have $m_b(Lg)$ measurements.

Based on nonlinear finite difference simulations for explosions in brittle high-velocity rock we conclude that spall should be a significant source of Lg. Other mechanisms such as near-source scattering may also be viable mechanisms for Lg excitation. A theoretical basis for yield estimation or discrimination based on Lg will require a better understanding of these mechanisms.

VII. REFERENCES

Aki, K, and P. G. Richards (1980). *QUANTITATIVE SEISMOLOGY Theory and Methods, Volume I,* Freeman, San Francisco, 556 pages.

Barker, T. G., and S. M. Day (1990). Spall Modeling of 2-D Axisymmetric Nonlinear Finite Difference Explosion Simulations, Scientific Report No. 3 submitted to Geophysics Laboratory, Hanscom Air Force Base, Ma 01731, S-CUBED Report SSS-TR-90-11550.

Barker, T. G., S. M. Day, K. L. McLaughlin, B. Shkoller, and J. L. Stevens. (1990). An Analysis of the Effects of Spall on Regional and Teleseismic Waveforms Using Two-Dimensional Numerical Modeling of Underground Explosions, Scientific Report No. 1 submitted Geophysics Laboratory, Hanscom Air Force Base, Ma 01731, S-CUBED Report SSS-TR-90-11536, GL-TR-90-0126.

Blandford, R. R, R. Hartenberger, and R. Naylor (1981). Regional Amplitude-Distance Relations, Discrimination and Detection, VSC-TR-81-15, Teledyne Geotech Report, Alexandria Va. 22314.

Day, S. M, N. Rimer, and J. T. Cherry (1983). Surface Waves from Underground Explosions with Spall: Analysis of Elastic and Nonlinear Source Models, *Bull. Seism. Soc. Am. 73,* 247-264.

Eisler, J. D., and F. Chilton (1964). Spalling of the Earth's Surface by Underground Nuclear Explosions, *J. Geophys. Res., 69,* 5285-5293.

Gupta, I. N., and R. R. Blandford (1983). A Mechanism for Generation of Short-Period Transverse Motion from Explosions, *Bull. Seism. Soc. Am., 73,* 571.

Johnson, L. R. (1988). Source Characteristics of Two Underground Nuclear Explosions, *Geophysical Journal, 95,* 15-30.

McLaughlin, K. L., T. G. Barker, S. M. Day, B. Shkoller, and J. L. Stevens (1988). Effects of Depth of Burial and Tectonic Release on Regional and Teleseismic Explosion Waveforms, AFGL-TR-88-0314, ADA207541, S-CUBED Report SSS-R-88-9844, La Jolla, Ca.

McLaughlin, K. L., and R. S. Jih (1986). Finite Difference Simulations of Rayleigh Wave Scattering by 2-D Rough Topography, AFGL-TR-86-0269, ADA179190, Teledyne Geotech, Alexandria, Va. 22314.

McLaughlin, K. L., and R. S. Jih (1987). Finite Difference Simulations of Rayleigh Wave Scattering by Shallow Heterogeneity, AFGL-TR-87-0322, ADA194961, Teledyne Geotech, Alexandria, Va. 22314.

Murphy, J. R., and T. J. Bennett (1983). A Discrimination Analysis of Short-Period Regional Seismic Data at Tonto Forest Observatory, *Bull. Seism. Soc. Am., 72,* 1351-1366.

Nuttli, O. W. (1986). Yield Estimates of Nevada Test Site Explosions Obtained From Seismic Lg Waves, *J. Geophys. Res. 91,* 2137-2151.

Patton, H. J. (1988). Source Models of the HARZER Explosion from Regional Observations of Fundamental-Mode and Higher Mode Surface Waves, *Bull. Seism. Soc. Am., 78,* 1133-1158.

Sobel, P. A. (1978). The Effect of Spall on mb and Ms, Teledyne Geotech Report, SDAC-TR-77-12, Dallas, Tx.

Springer, D. L., and R. L. Kinnaman, (1971) Seismic Source Summary for U.S. Underground Nuclear Explosion, 1961-1970, *Bull. Seism. Soc. Am., 61,* 1073-1098.

Springer, D. L., and R. L. Kinnaman, (1975) Seismic Source Summary for U.S. Underground Nuclear Explosion, 1971-1973, *Bull. Seism. Soc. Am., 65,* 343-349.

Stump, B. W. (1984). Resolving Point and Couples Forces in Explosion Modeling (Abstract), EOS, 65, 995.

Stump, B. W. (1985). Constraints on Explosive Sources with Spall from Near-Source Waveforms, *Bull. Seism. Soc. Am. 75,* 361-378.

Taylor, S. R., N. W. Sherman, and M. D. Denny, Spectral Discrimination Between NTS Explosions and Western Unites States Earthquakes at Regional Distances, *Bull. Seism. Soc. Am., 78,* 1563-1579.

Taylor, S. (1989). The Effects of Spall on Regional Seismograms, *Geophys. Res. Lett., 16,* 211-214.

Viecelli, J. A. (1973). Spallation and the Generation of Surface Waves by an Underground Explosion, *J. Geophys. Res. 78,* 2475-2487.

CONTRACTORS (United States)

Prof. Thomas Ahrens
Seismological Lab, 252-21
Division of Geological & Planetary Sciences
California Institute of Technology
Pasadena, CA 91125

Prof. Charles B. Archambeau
CIRES
University of Colorado
Boulder, CO 80309

Dr. Thomas C. Bache, Jr.
Science Applications Int'l Corp.
10260 Campus Point Drive
San Diego, CA 92121 (2 copies)

Prof. Muawia Barazangi
Institute for the Study of the Continent
Cornell University
Ithaca, NY 14853

Dr. Douglas R. Baumgardt
ENSCO, Inc
5400 Port Royal Road
Springfield, VA 22151-2388

Prof. Jonathan Berger
IGPP, A-025
Scripps Institution of Oceanography
University of California, San Diego
La Jolla, CA 92093

Dr. Lawrence J. Burdick
Woodward-Clyde Consultants
566 El Dorado Street
Pasadena, CA 91109-3245

Dr. Karl Coyner
New England Research, Inc.
76 Olcott Drive
White River Junction, VT 05001

Prof. Vernon F. Cormier
Department of Geology & Geophysics
U-45, Room 207
The University of Connecticut
Storrs, CT 06268

Professor Anton W. Dainty
Earth Resources Laboratory
Massachusetts Institute of Technology
42 Carleton Street
Cambridge, MA 02142

Prof. Steven Day
Department of Geological Sciences
San Diego State University
San Diego, CA 92182

Dr. Zoltan A. Der
ENSCO, Inc.
5400 Port Royal Road
Springfield, VA 22151-2388

Prof. John Ferguson
Center for Lithospheric Studies
The University of Texas at Dallas
P.O. Box 830688
Richardson, TX 75083-0688

Prof. Stanley Flatte
Applied Sciences Building
University of California
Santa Cruz, CA 95064

Dr. Alexander Florence
SRI International
333 Ravenswood Avenue
Menlo Park, CA 94025-3493

Prof. Henry L. Gray
Vice Provost and Dean
Department of Statistical Sciences
Southern Methodist University
Dallas, TX 75275

Dr. Indra Gupta
Teledyne Geotech
314 Montgomery Street
Alexandria, VA 22314

Prof. David G. Harkrider
Seismological Laboratory
Division of Geological & Planetary Sciences
California Institute of Technology
Pasadena, CA 91125

Prof. Donald V. Helmberger
Seismological Laboratory
Division of Geological & Planetary Sciences
California Institute of Technology
Pasadena, CA 91125

Prof. Eugene Herrin
Institute for the Study of Earth and Man
GeophysicalLaboratory
Southern Methodist University
Dallas, TX 75275

Prof . Robert B. Herrmann
Department of Earth & Atmospheric Sciences
St. Louis University
St. Louis, MO 63156

Prof. Bryan Isacks
Cornell University
Department of Geological Sciences
SNEE Hall
Ithaca, NY 14850

Dr. Rong-Song Jih
Teledyne Geotech
314 Montgomery Street
Alexandria, VA 22314

Prof. Lane R. Johnson
Seismographic Station
University of California
Berkeley, CA 94720

Prof. Alan Kafka
Department of Geology & Geophysics
Boston College
Chestnut Hill, MA 02167

Dr. Richard LaCoss
MIT-Lincoln Laboratory
M-200B
P. O. Box 73
Lexington, MA 02173-0073 (3 copies)

Prof Fred K. Lamb
University of Illinois at Urbana-Champaign
Department of Physics
1110 West Green Street
Urbana, IL 61801

Prof. Charles A. Langston
Geosciences Department
403 Deike Building
The Pennsylvania State University
University Park, PA 16802

Prof. Thorne Lay
Institute of Tectonics
Earth Science Board
University of California, Santa Cruz
Santa Cruz, CA 95064

Prof. Arthur Lerner-Lam
Lamont-Doherty Geological Observatory
of Columbia University
Palisades, NY 10964

Dr. Christopher Lynnes
Teledyne Geotech
314 Montgomery Street
Alexandria, VA 22314

Prof. Peter Malin
University of California at Santa Barbara
Institute for Crustal Studies
Santa Barbara, CA 93106

Dr. Randolph Martin, III
New England Research, Inc.
76 Olcott Drive
White River Junction, VT 05001

Dr. Gary McCartor
Mission Research Corporation
735 State Street
P.O. Drawer 719
Santa Barbara, CA 93102 (2 copies)

Prof. Thomas V. McEvilly
Seismographic Station
University of California
Berkeley, CA 94720

Dr. Keith L. McLaughlin
S-CUBED
A Division of Maxwell Laboratory
P.O. Box 1620
La Jolla, CA 92038-1620

Prof. William Menke
Lamont-Doherty Geological Observatory
of Columbia University
Palisades, NY 10964

Stephen Miller
SRI International
333 Ravenswood Avenue
Box AF 116
Menlo Park, CA 94025-3493

Prof. Bernard Minster
IGPP, A-025
Scripps Institute of Oceanography
University of California, San Diego
La Jolla, CA 92093

Prof. Brian J. Mitchell
Department of Earth & Atmospheric Sciences
St. Louis University
St. Louis, MO 63156

Mr. Jack Murphy
S-CUBED, A Division of Maxwell Laboratory
11800 Sunrise Valley Drive
Suite 1212
Reston, VA 22091 (2 copies)

Dr. Bao Nguyen
GL/LWH
Hanscom AFB, MA 01731-5000

Prof. John A. Orcutt
IGPP, A-025
Scripps Institute of Oceanography
University of California, San Diego
La Jolla, CA 92093

Prof. Keith Priestley
University of Cambridge
Bullard Labs, Dept. of Earth Sciences
Madingley Rise, Madingley Rd.
Cambridge CB3 OEZ, ENGLAND

Prof. Paul G. Richards
L-210
Lawrence Livermore National Laboratory
Livermore, CA 94550

Dr. Wilmer Rivers
Teledyne Geotech
314 Montgomery Street
Alexandria, VA 22314

Prof. Charles G. Sammis
Center for Earth Sciences
University of Southern California
University Park
Los Angeles, CA 90089-0741

Prof. Christopher H. Scholz
Lamont-Doherty Geological Observatory
of Columbia University
Palisades, NY 10964

Thomas J. Sereno, Jr.
Science Application Int'l Corp.
10260 Campus Point Drive
San Diego, CA 92121

Prof. David G. Simpson
Lamont-Doherty Geological Observatory
of Columbia University
Palisades, NY 10964

Dr. Jeffrey Stevens
S-CUBED
A Division of Maxwell Laboratory
P.O. Box 1620
La Jolla, CA 92038-1620

Prof. Brian Stump
Institute for the Study of Earth & Man
Geophysical Laboratory
Southern Methodist University
Dallas, TX 75275

Prof. Jeremiah Sullivan
University of Illinois at Urbana-Champaign
Department of Physics
1110 West Green Street
Urbana, IL 61801

Prof. Clifford Thurber
University of Wisconsin-Madison
Department of Geology & Geophysics
1215 West Dayton Street
Madison, WS 53706

Prof. M. Nafi Toksoz
Earth Resources Lab
Massachusetts Institute of Technology
42 Carleton Street
Cambridge, MA 02142

Prof. John E. Vidale
University of California at Santa Cruz
Seismological Laboratory
Santa Cruz, CA 95064

Prof. Terry C. Wallace
Department of Geosciences
Building #77
University of Arizona
Tucson, AZ 85721

Dr. Raymond Willeman
GL/LWH
Hanscom AFB, MA 01731-5000

Dr. Lorraine Wolf
GL/LWH
Hanscom AFB, MA 01731-5000

Dr. Monem Abdel-Gawad
Rockwell International Science Center
1049 Camino Dos Rios
Thousand Oaks, CA 91360

Prof. Keiiti Aki
Center for Earth Sciences
University of Southern California
University Park
Los Angeles, CA 90089-0741

Prof. Shelton S. Alexander
Geosciences Department
403 Deike Building
The Pennsylvania State University
University Park, PA 16802

Dr. Kenneth Anderson
BBNSTC
Mail Stop 14/1B
Cambridge, MA 02238

Dr. Ralph Archuleta
Department of Geological Sciences
University of California at Santa Barbara
Santa Barbara, CA 93102

J. Barker
Department of Geological Sciences
State University of New York
at Binghamton
Vestal, NY 13901

Dr. T.J. Bennett
S-CUBED
A Division of Maxwell Laboratory
11800 Sunrise Valley Drive, Suite 1212
Reston, VA 22091

Mr. William J. Best
907 Westwood Drive
Vienna, VA 22180

Dr. N. Biswas
Geophysical Institute
University of Alaska
Fairbanks, AK 99701

Dr. G.A. Bollinger
Department of Geological Sciences
Virginia Polytechnical Institute
21044 Derring Hall
Blacksburg, VA 24061

Dr. Stephen Bratt
Center for Seismic Studies
1300 North 17th Street
Suite 1450
Arlington, VA 22209

Michael Browne
Teledyne Geotech
3401 Shiloh Road
Garland, TX 75041

Mr. Roy Burger
1221 Serry Road
Schenectady, NY 12309

Dr. Robert Burridge
Schlumberger-Doll Research Center
Old Quarry Road
Ridgefield, CT 06877

Dr. Jerry Carter
Rondout Associates
P.O. Box 224
Stone Ridge, NY 12484

Dr. W. Winston Chan
Teledyne Geotech
314 Montgomery Street
Alexandria, VA 22314-1581

Dr. Theodore Cherry
Science Horizons, Inc.
710 Encinitas Blvd., Suite 200
Encinitas, CA 92024 (2 copies)

Prof. Jon F. Claerbout
Department of Geophysics
Stanford University
Stanford, CA 94305

Prof. Robert W. Clayton
Seismological Laboratory
Division of Geological & Planetary Sciences
California Institute of Technology
Pasadena, CA 91125

Prof. F. A. Dahlen
Geological and Geophysical Sciences
Princeton University
Princeton, NJ 08544-0636

Prof. Adam Dziewonski
Hoffman Laboratory
Harvard University
20 Oxford St
Cambridge, MA 02138

Prof. John Ebel
Department of Geology & Geophysics
Boston College
Chestnut Hill, MA 02167

Eric Fielding
SNEE Hall
INSTOC
Cornell University
Ithaca, NY 14853

Prof. Donald Forsyth
Department of Geological Sciences
Brown University
Providence, RI 02912

Dr. Cliff Frolich
Institute of Geophysics
8701 North Mopac
Austin, TX 78759

Prof. Art Frankel
Mail Stop 922
Geological Survey
790 National Center
Reston, VA 22092

Dr. Anthony Gangi
Texas A&M University
Department of Geophysics
College Station, TX 77843

Dr. Freeman Gilbert
Inst. of Geophysics & Planetary Physics
University of California, San Diego
P.O. Box 109
La Jolla, CA 92037

Mr. Edward Giller
Pacific Sierra Research Corp.
1401 Wilson Boulevard
Arlington, VA 22209

Dr. Jeffrey W. Given
Sierra Geophysics
11255 Kirkland Way
Kirkland, WA 98033

Prof. Stephen Grand
University of Texas at Austin
Department of Geological Sciences
Austin, TX 78713-7909

Prof. Roy Greenfield
Geosciences Department
403 Deike Building
The Pennsylvania State University
University Park, PA 16802

Dan N. Hagedorn
Battelle
Pacific Northwest Laboratories
Battelle Boulevard
Richland, WA 99352

Kevin Hutchenson
Department of Earth Sciences
St. Louis University
3507 Laclede
St. Louis, MO 63103

Prof. Thomas H. Jordan
Department of Earth, Atmospheric
and Planetary Sciences
Massachusetts Institute of Technology
Cambridge, MA 02139

Robert C. Kemerait
ENSCO, Inc.
445 Pineda Court
Melbourne, FL 32940

William Kikendall
Teledyne Geotech
3401 Shiloh Road
Garland, TX 75041

Prof. Leon Knopoff
University of California
Institute of Geophysics & Planetary Physics
Los Angeles, CA 90024

Prof. L. Timothy Long
School of Geophysical Sciences
Georgia Institute of Technology
Atlanta, GA 30332

Prof. Art McGarr
Mail Stop 977
Geological Survey
345 Middlefield Rd.
Menlo Park, CA 94025

Dr. George Mellman
Sierra Geophysics
11255 Kirkland Way
Kirkland, WA 98033

Prof. John Nabelek
College of Oceanography
Oregon State University
Corvallis, OR 97331

Prof. Geza Nagy
University of California, San Diego
Department of Ames, M.S. B-010
La Jolla, CA 92093

Prof. Amos Nur
Department of Geophysics
Stanford University
Stanford, CA 94305

Prof. Jack Oliver
Department of Geology
Cornell University
Ithaca, NY 14850

Prof. Robert Phinney
Geological & Geophysical Sciences
Princeton University
Princeton, NJ 08544-0636

Dr. Paul Pomeroy
Rondout Associates
P.O. Box 224
Stone Ridge, NY 12484

Dr. Jay Pulli
RADIX System, Inc.
2 Taft Court, Suite 203
Rockville, MD 20850

Dr. Norton Rimer
S-CUBED
A Division of Maxwell Laboratory
P.O. Box 1620
La Jolla, CA 92038-1620

Prof. Larry J. Ruff
Department of Geological Sciences
1006 C C. Little Building
University of Michigan
Ann Arbor, MI 48109-1063

Dr. Richard Sailor
TASC Inc.
55 Walkers Brook Drive
Reading, MA 01867

John Sherwin
Teledyne Geotech
3401 Shiloh Road
Garland, TX 75041

Prof. Robert Smith
Department of Geophysics
University of Utah
1400 East 2nd South
Salt Lake City, UT 84112

Dr. Stewart Smith
IRIS Inc.
1616 North Fort Myer Drive
Suite 1440
Arlington, VA 22209

Dr. George Sutton
Rondout Associates
P.O. Box 224
Stone Ridge, NY 12484

Prof. L. Sykes
Lamont-Doherty Geological Observatory
of Columbia University
Palisades, NY 10964

Prof. Pradeep Talwani
Department of Geological Sciences
University of South Carolina
Columbia, SC 29208

Prof. Ta-liang Teng
Center for Earth Sciences
University of Southern California
University Park
Los Angeles, CA 90089-0741

Dr. R.B. Tittmann
Rockwell International Science Center
1049 Camino Dos Rios
P.O. Box 1085
Thousand Oaks, CA 91360

Dr. Gregory van der Vink
IRIS, Inc.
1616 North Fort Myer Drive
Suite 1440
Arlington, VA 22209

Professor Daniel Walker
University of Hawaii
Institute of Geophysics
Honolulu, HI 96822

William R. Walter
Seismological Laboratory
University of Nevada
Reno, NV 89557

Dr. Gregory Wojcik
Weidlinger Associates
4410 El Camino Real
Suite 110
Los Altos, CA 94022

Prof. John H. Woodhouse
Hoffman Laboratory
Harvard University
20 Oxford St.
Cambridge, MA 02138

Prof. Francis T. Wu
Department of Geological Sciences
State University of New York
at Binghamton
Vestal, NY 13901

Dr. Gregory B. Young
ENSCO, Inc.
5400 Port Royal Road
Springfield, VA 22151-2388

Dr. Ralph Alewine III
DARPA/NMRO
1400 Wilson Boulevard
Arlington, VA 22209-2308

Mr. James C. Battis
GL/LWH
Hanscom AFB, MA 01731-5000

Dr. Robert Blandford
DARPA/NMRO
1400 Wilson Boulevard
Arlington, VA 22209-2308

Eric Chael
Division 9241
Sandia Laboratory
Albuquerque, NM 87185

Dr. John J. Cipar
GL/LWH
Hanscom AFB, MA 01731-5000

Mr. Jeff Duncan
Office of Congressman Markey
2133 Rayburn House Bldg.
Washington, DC 20515

Dr. Jack Evernden
USGS - Earthquake Studies
345 Middlefield Road
Menlo Park, CA 94025

Art Frankel
USGS
922 National Center
Reston, VA 22092

Dr. T. Hanks
USGS
Nat'l Earthquake Research Center
345 Middlefield Road
Menlo Park, CA 94025

Dr. James Hannon
Lawrence Livermore Nat'l Laboratory
P.O. Box 808
Livermore, CA 94550

Paul Johnson
ESS-4, Mail Stop J979
Los Alamos National Laboratory
Los Alamos, NM 87545

Janet Johnston
GL/LWH
Hanscom AFB, MA 01731-5000

Dr. Katharine Kadinsky-Cade
GL/LWH
Hanscom AFB, MA 01731-5000

Ms. Ann Kerr
IGPP, A-025
Scripps Institute of Oceanography
University of California, San Diego
La Jolla, CA 92093

Dr. Max Koontz
US Dept of Energy/DP 5
Forrestal Building
1000 Independence Avenue
Washington, DC 20585

Dr. W.H.K. Lee
Office of Earthquakes, Volcanoes,
& Engineering
345 Middlefield Road
Menlo Park, CA 94025

Dr. William Leith
U.S. Geological Survey
Mail Stop 928
Reston, VA 22092

Dr. Richard Lewis
Director, Earthquake Engineering & Geophysics
U.S. Army Corps of Engineers
Box 631
Vicksburg, MS 39180

James F. Lewkowicz
GL/LWH
Hanscom AFB, MA 01731-5000

Mr. Alfred Lieberman
ACDA/VI-OA'State Department Bldg
Room 5726
320 - 21st Street, NW
Washington, DC 20451

Stephen Mangino
GL/LWH
Hanscom AFB, MA 01731-5000

Dr. Robert Masse
Box 25046, Mail Stop 967
Denver Federal Center
Denver, CO 80225

Art McGarr
U.S. Geological Survey, MS-977
345 Middlefield Road
Menlo Park, CA 94025

Richard Morrow
ACDA/VI, Room 5741
320 21st Street N.W
Washington, DC 20451

Dr. Keith K. Nakanishi
Lawrence Livermore National Laboratory
P.O. Box 808, L-205
Livermore, CA 94550

Dr. Carl Newton
Los Alamos National Laboratory
P.O. Box 1663
Mail Stop C335, Group ESS-3
Los Alamos, NM 87545

Dr. Kenneth H. Olsen
Los Alamos Scientific Laboratory
P.O. Box 1663
Mail Stop C335, Group ESS-3
Los Alamos, NM 87545

Howard J. Patton
Lawrence Livermore National Laboratory
P.O. Box 808, L-205
Livermore, CA 94550

Mr. Chris Paine
Office of Senator Kennedy
SR 315
United States Senate
Washington, DC 20510

Colonel Jerry J. Perrizo
AFOSR/NP, Building 410
Bolling AFB
Washington, DC 20332-6448

Dr. Frank F. Pilotte
HQ AFTAC/TT
Patrick AFB, FL 32925-6001

Katie Poley
CIA-OSWR/NED
Washington, DC 20505

Mr. Jack Rachlin
U.S. Geological Survey
Geology, Rm 3 C136
Mail Stop 928 National Center
Reston, VA 22092

Dr. Robert Reinke
WL/NTESG
Kirtland AFB, NM 87117-6008

Dr. Byron Ristvet
HQ DNA, Nevada Operations Office
Attn: NVCG
P.O. Box 98539
Las Vegas, NV 89193

Dr. George Rothe
HQ AFTAC/TGR
Patrick AFB, FL 32925-6001

Dr. Alan S. Ryall, Jr.
DARPA/NMRO
1400 Wilson Boulevard
Arlington, VA 22209-2308

Dr. Michael Shore
Defense Nuclear Agency/SPSS
6801 Telegraph Road
Alexandria, VA 22310

Dr. Albert Smith
Los Alamos National Laboratory
L-205
P. O. Box 808
Livermore, CA 94550

Donald L. Springer
Lawrence Livermore National Laboratory
L-205
P. O. Box 808
Livermore , CA 94550

Mr. Charles L. Taylor
GL/LWG
Hanscom AFB, MA 01731-5000

Mr. Steven R. Taylor
Lawrence Livermore National Laboratory
L-205
P. O. Box 808
Livermore, CA 94550

Dr. Eileen Vergino
Lawrence Livermore National Laboratory
L-205
P. O. Box 808
Livermore, CA 94550

Dr. Thomas Weaver
Los Alamos National Laboratory
P.O. Box 1663, Mail Stop C335
Los Alamos, NM 87545

J.J. Zucca
Lawrence Livermore National Laboratory
P. O. Box 808
Livermore, CA 94550

GL/SULL
Research Library
Hanscom AFB , MA 01731-5000 (2 copies)

Secretary of the Air Force
(SAFRD)
Washington, DC 20330

Office of the Secretary Defense
DDR & E
Washington, DC 20330

HQ DNA
Attn: Technical Library
Washington, DC 20305

DARPA/RMO/RETRIEVAL
1400 Wilson Boulevard
Arlington, VA 22209

DARPA/RMO/Security Office
1400 Wilson Boulevard
Arlington, VA 22209

Geophysics Laboratory
Attn: XO
Hanscom AFB, MA 01731-5000

Geophysics Laboratory
Attn: LW
Hanscom AFB, MA 01731-5000

DARPA/PM
1400 Wilson Boulevard
Arlington, VA 22209

Defense Technical Information Center
Cameron Station
Alexandria, VA 22314 (5 copies)

Defense Intelligence Agency
Directorate for Scientific
& Technical IntelligenceAttn: DT1B
Washington, DC 20340-6158

AFTAC/CA
(STINFO)
Patrick AFB, FL 32925-6001

TACTEC
Battelle Memorial Institute
505 King Avenue
Columbus, OH 43201 (Final Report Only)

Dr. Ramon Cabre, S.J.
Observatorio San Calixto
Casilla 5939
La Paz, Bolivia

Prof. Hans-Peter Harjes
Institute for Geophysik
Ruhr University/Bochum
P.O. Box 102148
4630 Bochum 1, FRG

Prof. Eystein Husebye
NTNF/NORSAR
P.O. Box 51
N-2007 Kjeller, NORWAY

Prof. Brian L.N. Kennett
Research School of Earth Sciences
Institute of Advanced Studies
G.P.O. Box 4
Canberra 2601, AUSTRALIA

Dr. Bernard Massinon
Societe Radiomana
27 rue Claude Bernard
75005 Paris, FRANCE (2 Copies)

Dr. Pierre Mecheler
Societe Radiomana
27 rue Claude Bernard
75005 Paris, FRANCE

Dr. Svein Mykkeltveit
NTNF/NORSAR
P.O. Box 51
N-2007 Kjeller, NORWAY

FOREIGN (Others)

Dr. Peter Basham
Earth Physics Branch
Geological Survey of Canada
1 Observatory Crescent
Ottawa, Ontario, CANADA K1A 0Y3

Dr. Eduard Berg
Institute of Geophysics
University of Hawaii
Honolulu, HI 96822

Dr. Michel Bouchon
I.R.I.G.M.-B.P. 68
38402 St. Martin D'Heres
Cedex, FRANCE

Dr. Hilmar Bungum
NTNF/NORSAR
P.O. Box 51
N-2007 Kjeller, NORWAY

Dr. Michel Campillo
Observatoire de Grenoble
I.R.I.G.M.-B.P. 53
38041 Grenoble, FRANCE

Dr. Kin Yip Chun
Geophysics Division
Physics Department
University of Toronto
Ontario, CANADA M5S 1A7

Dr. Alan Douglas
Ministry of Defense
Blacknest, Brimpton
Reading RG7-4RS, UNITED KINGDOM

Dr. Roger Hansen
NTNF/NORSAR
P.O. Box 51
N-2007 Kjeller, NORWAY

Dr. Manfred Henger
Federal Institute for Geosciences & Nat'l Res.
Postfach 510153
D-3000 Hanover 51, FRG

Ms. Eva Johannisson
Senior Research Officer
National Defense Research Inst.
P.O. Box 27322
S-102 54 Stockholm, SWEDEN

Dr. Fekadu Kebede
Seismological Section
Box 12019
S-750 Uppsala, SWEDEN

Dr. Tormod Kvaerna
NTNF/NORSAR
P.O. Box 51
N-2007 Kjeller, NORWAY

Dr. Peter Marshal
Procurement Executive
Ministry of Defense
Blacknest, Brimpton
Reading FG7-4RS, UNITED KINGDOM

Prof. Ari Ben-Menahem
Department of Applied Mathematics
Weizman Institute of Science
Rehovot, ISRAEL 951729

Dr. Robert North
Geophysics Division
Geological Survey of Canada
1 Observatory Crescent
Ottawa, Ontario, CANADA K1A 0Y3

Dr. Frode Ringdal
NTNF/NORSAR
P.O. Box 51
N-2007 Kjeller, NORWAY

Dr. Jorg Schlittenhardt
Federal Institute for Geosciences & Nat'l Res.
Postfach 510153
D-3000 Hannover 51, FEDERAL REPUBLIC OF GERMANY